Mechanism of Naphthoquinone Selectivity of Thymidylate Synthase ThyX

Hannu Myllykallio, Hubert F Becker, Alexey Aleksandrov

Journal Pre-proof

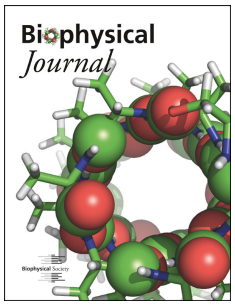

Mechanism of naphthoquinone selectivity of thymidylate synthase ThyX

Hannu Myllykallio, Hubert F. Becker, Alexey Aleksandrov

PII: S0006-3495(20)30889-4

DOI: https://doi.org/10.1016/j.bpj.2020.10.042

Reference: BPJ 10670

To appear in: *Biophysical Journal*

Received Date: 28 August 2020

Accepted Date: 30 October 2020

Please cite this article as: Myllykallio H, Becker HF, Aleksandrov A, Mechanism of naphthoquinone selectivity of thymidylate synthase ThyX, *Biophysical Journal* (2020), doi: https://doi.org/10.1016/j.bpj.2020.10.042.

Mechanism of naphthoquinone selectivity of thymidylate synthase ThyX

Hannu Myllykallio[1*], Hubert F. Becker[1, 2], and Alexey Aleksandrov[1*]

[1]Laboratoire d'Optique et Biosciences (CNRS UMR7645, INSERM U1182), Ecole Polytechnique, Institut polytechnique de Paris, F-91128 Palaiseau, France.

[2]Sorbonne Université, Faculté des Sciences et Ingénierie, 75005, Paris, France.

*__Corresponding authors__: Alexey.Aleksandrov@polytechnique.edu, Hannu.Myllykallio@polytechnique.edu

Running title: *Mechanism of Naphthoquinone Selectivity of Thymidylate Synthase ThyX*

Keywords: Molecular dynamics; protonation free energy; binding free energy; thymidylate synthase ThyX; flavin; naphthoquinone, enzyme inhibitors

ABSTRACT

Naphthoquinones (NQs) are natural and synthetic compounds with a wide range of biological activities commonly attributed to their redox activity and/or chemical reactivity. However, genetic and biochemical experiments have recently demonstrated that 2-hydroxy-NQs (2-OH-NQs) act as highly specific non-covalent inhibitors of the essential bacterial thymidylate synthase ThyX in a cellular context. We used biochemical experiments and molecular dynamics simulations to elucidate the selective inhibition mechanism of NQ inhibitors of ThyX from *Mycobacterium tuberculosis* (*Mtb*). Free energy simulations rationalized how ThyX recognizes the natural substrate dUMP in the N3 ionized form using an arginine, Arg199 in *Mtb*. The results further demonstrated that 2-OH-NQ, similarly to dUMP, binds to ThyX in the ionized form and the strong and selective binding of 2-OH-NQ to ThyX is also explained by electrostatic interactions with Arg199. The stronger binding of the close analog 5F-dUMP to ThyX and its inhibitory properties compared to dUMP were explained by the stronger acidity of the uracil N3 atom. Our results, therefore, revealed that the ionization of 2-OH-NQs drives their biological activities by mimicking the interactions with the natural substrate. Our observations encourage the rational design of optimized ThyX inhibitors that ultimately may serve as antibiotics.

Statement of Significance

In this work, we use experimental and simulation techniques to elucidate the mechanism of naphthoquinone (NQ) selectivity of bacterial thymidylate synthase, ThyX. Our observations encourage the rational design of optimized ThyX inhibitors mimicking dUMP that ultimately may serve as antibiotics. To demonstrate the mechanistic concept, benzoate was identified based on these insights as an inhibitor of ThyX. Finally, we would like to stress that these observations are of general interest for a wide range of experimental scientists working on the different aspects of biological activities of NQs.

INTRODUCTION

Naphthoquinones (NQs) are important secondary metabolites and represent the most common quinones found in nature. NQs are also an essential part of many drugs including anticancer,[1-3] antibacterial,[4-7] antifungal,[8-9], and anti-inflammatory[10-11] agents. Biological activities of NQs are widely associated with their non-specific redox activity and/or chemical reactivity.[3, 12] Recently, through experimental screening assays, 1,4-naphthoquinone (NQ) derivatives emerged as selective and potent inhibitors of the bacterial ThyX family of thymidylate synthases [E.C. 2.1.1.148; flavin-dependent thymidylate synthase (FDTS)].[5] Surprisingly, no redox cycling or covalent binding of NQs to the ThyX active site was observed.[5] This raises the question of the molecular mechanism of the selective inhibition of ThyX by these compounds.

Thymidylate synthases (TS) are involved in the *de novo* production of an essential DNA precursor (thymidylate, dTMP) during DNA replication.[13] In approximately 30% of bacteria, including the human pathogens *Mycobacterium tuberculosis*, *Bacillus anthracis*, and *Helicobacter pylori*, thymidylate synthesis is accomplished by the ThyX family of thymidylate synthases. In humans, TS is encoded by gene *TYMS* (ThyA family of thymidylate synthases, EC number 2.1.1.1.45). ThyX proteins have no sequence similarity to the human thymidylate synthase ThyA and use a flavin adenine dinucleotide (FAD) cofactor to achieve the required methylation reaction.[14] ThyX from different organisms share a common architecture[15-17] and are structurally different from ThyA. The current consensus on the chemical reaction mechanisms of the different TS families include noticeable differences in chemical strategies for converting dUMP to dTMP.[14, 18] Instead of a nucleophilic attack at the C6 of dUMP as in ThyA, ThyX activates C5 by ionization of the uracil N3 of dUMP as demonstrated by the crystal structures of the dUMP: ThyX complex, in which the NH nitrogen of the conserved Arg199 (Arg199, Arg182, and Arg174 in *Mtb*, *Paramecium bursaria* chlorella virus-1 (PBCV-1) and *Thermotoga maritima* ThyX numbering, respectively) positioned 2.8 Å away from N3 of dUMP as shown in Figure 1. This result was corroborated by nuclear magnetic resonance (NMR) experiments.[19]

The lack of ThyX in humans, the high sequence and structural conservation of the different ThyX orthologs from different bacterial organisms, and its crucial cellular role using a unique reaction mechanism make ThyX a promising target for antibacterial drug development.[5, 20-22] Importantly, even if *Mtb* carries genes for both TS families, only ThyX is essential for its growth.[23] Several experimental studies have been devoted to the discovery of inhibitors of ThyX.[4-5, 20-21, 24-29] Some ThyX inhibitors act as selective inhibitors of *Mtb* ThyX in live cells,[25, 29] without forming a covalent bond with the enzyme. Among the identified compounds, many are based on the 2-hydroxy-1,4-naphthoquinone (2-OH-NQ) scaffold, with the inhibitory activity attributed to the efficient competitive binding with dUMP characterized by K_d values in the nano-molar range. These compounds have potent antibacterial activity against *H. pylori* but do not interfere with the function of human thymidylate synthase.[4]

Here we exploited the structure of the previously determined ThyX in complex with a 2-OH-NQ derivative, 2-hydroxy-3-(4-methoxybenzyl)naphthalene-1,4-dione (C8-C1), shown in Figure 1, to rationalize the mechanism of the observed inhibition. Atomistic molecular dynamics simulations and free-energy calculations, supported by experimental spectroscopy data, indicated that naphthoquinones inhibit ThyX by mimicking interactions of the natural dUMP substrate required for the activation of C5 of the nucleotide substrate. Moreover, the 2-OH-NQ inhibitors are deprotonated at physiological conditions at the 2-OH group in the ThyX complex and have a very similar mode of interaction with the catalytic arginine residue participating in deprotonation of dUMP. Based on these insights, benzoate was identified as a new inhibitor scaffold candidate of ThyX. These novel atomistic details provided a deeper understanding of the inhibitory mechanism and will facilitate the rational design of new antibiotics exploiting the unique reaction mechanism of ThyX enzymes.

RESULTS

ThyX recognizes the ionized form of the natural dUMP substrate

The protonation state of dUMP in complex with ThyX was first examined using a combination of experimental and computational approaches to investigate if the ionization state of dUMP and ThyX can modulate the strength of interactions between the ligand and protein.[19] It was demonstrated by crystallographic experiments that dUMP is deprotonated on N3 in complex with ThyX from *T. maritima*.[30] Subsequent NMR experiments provided further evidence that the ionization of dUMP is associated with interactions with Arg199, however, no pK_a estimate of N3 was obtained.[19] Using ThyX from *Mtb*, we computed the deprotonation free energy at the N3 nitrogen of dUMP in the protein complex relative to the solvent. Table 1 summarizes the results. The computed deprotonation free energy at the N3 nitrogen of dUMP in ThyX relative to the solvent is -8.6 kcal·mol^{-1} (standard deviation (SD): 0.7 kcal·mol^{-1}) favoring the deprotonated state of uracil. Combining this value with the experimental pK_a of N3 of dUMP in a solution of 9.3 units,[31] the total deprotonation free energy is 6.8 kcal·mol^{-1}, which corresponds to pK_a of dUMP in ThyX of 3 units in agreement with the crystallographic experiments and previous NMR measurements.[19] The unusually low pK_a of uracil of dUMP in ThyX is explained by strong electrostatic interactions between the guanidinium cations of Arg199 and Arg107 and the ionized uracil ring, as shown in Figure 1. Previously it was shown that the Arg174Ala mutation (Arg199Ala in *Mtb*) increases the disassociation constant of dUMP from ThyX from *T. maritima* from 0.03 to 109 μM.[19] This corresponds to the binding free energy difference of 4.8 kcal·mol^{-1}. However, the comparison of this value with 6.8 kcal·mol^{-1} obtained in this work for the binding free energy difference between the protonated and deprotonated forms should be made with caution. Indeed, these values correspond to the different processes, i.e. the difference in the binding of two forms of the ligand to the same protein, and the difference in binding of two forms of the ligand to the wild-type protein and the Arg174Ala mutant, which are obviously not equivalent.

Table 1. Computed free energy in kcal·mol^{-1} in the solvent and the ThyX complex using the alchemical free energy/thermodynamic integration method. The standard error was estimated from three forward-backward runs of 144 ns total.

	ΔG	ΔΔG

	Solvent	Protein	
dUMP 3N-H→3N$^-$ (Arg199-H$^+$)	-90.8±0.1	-99.4±0.7	-8.6±0.7
C8-C1 2-OH→2-O$^-$ (Arg199-H$^+$)	-53.8±0.2	-61.9±0.2	-8.1±0.3
C8-C1 2-OH→2-O$^-$ (Arg199$^{(0)}$)	-53.8±0.2	-52.2±0.7	1.6±0.7
Arg199-H$^+$→ Arg199$^{(0)}$ (C8-C1 2-O$^-$)	32.7±0.3	38.3±2.4	5.6±2.5
Arg199-H$^+$→ Arg199$^{(0)}$ (no C8-C1)	32.7±0.3	33.6±1.2	0.9±1.3

Figure 1. (A) A close-up view of the binding pocket of 5-fluoro-2'-deoxyuridine 5'-monophosphate (5F-dUMP) (crystal structure 3GWC[32]) in the *Mtb* ThyX enzyme, and (B) the 2-hydroxy-3-(4-methoxybenzyl)naphthalene-1,4-dione ~~(C8-C1)~~ ligand in the PBCV-1 enzyme, (crystal structure 4FZB[5]). The most important interactions are indicated by dashed lines; the residue numbering for the structure with 5F-dUMP and C8-C1 corresponds to ThyX from *Mtb* and PBCV-1, respectively. The corresponding residues for *Mtb* for the C8-C1 structure are given in parentheses. The pK_a values in the solvent for C8-C1 and 5F-dUMP were from this work and ref[33], respectively. The figure was prepared with the Pymol and MarvinSketch programs.[34-35]

5-fluoro dUMP and dUMP binding to ThyX

The significantly large protonation free energy also demonstrates that binding of the protonated form of uracil to ThyX can be neglected. Based on this observation, we propose that a ligand similar to dUMP, but with a lower pK_a of site N3, in principle, can bind more strongly than the natural dUMP ligand, since less energy is required for deprotonation upon binding to ThyX. One of such dUMP analogs is 5-fluoro-2'-deoxyuridine 5'-monophosphate ~~(5F-dUMP)~~, which has a fluoro group at position 5, and the pK_a of the N3 site of 8 units.[33] To experimentally compare the binding of dUMP and 5F-dUMP to *Mtb* ThyX, the dissociation constant K_d was measured using spectrophotometric titrations. In particular, the UV-vis absorbance spectrum change at 450 nm was recorded at different concentrations of the ligand to investigate the nucleotide-binding, in agreement with the previous study.[19] The effect of the ligand addition on the absorbance at 450 nm is shown in Figure 2. The fitted K_d using Equation 1 and two independent measurements is 10.8 and 3.8 μM for dUMP and 5F-dUMP, respectively. Using $\Delta\Delta G = RTLn(K_d^{5F-dUMP}/K_d^{dUMP})$, where R is the gas constant and T is temperature, the binding free energy difference $\Delta\Delta G$ is 0.6 kcal·mol^{-1}. This binding free energy difference includes two contributions, first, due to the difference in interactions of the ionized forms of the ligands with the protein, and second, due to the difference in the deprotonation free energy at N3 in the solvent. The binding free energy difference of the N3 deprotonated form of the ligands computed using the alchemical free energy method is -0.8 (SD 0.2) kcal·mol^{-1} favoring dUMP binding over 5F-dUMP. Combining this value with the difference in the free energy needed to deprotonate dUMP and 5F-dUMP in the solvent, the total binding free energy difference is -1.0 kcal·mol^{-1} favoring 5F-dUMP binding in good agreement with the spectrophotometric experiments. Thus, the deprotonated form of 5F-dUMP binds weaker than the ionized form of dUMP, but the stronger acidity of 5F-dUMP makes it a stronger binder to ThyX overall.

Figure 2. Upper panel: spectrophotometric titration of dUMP and 5F-dUMP. The flavin concentration was 16 μM. Data are averaged over two independent measurements. The fitted K_d averaged over two independent measurements is 10.8 and 3.8 μM for dUMP and 5F-dUMP, respectively. Lower panel: absorbance spectra of C8-C1 in aqueous solution at different pH; inset panel: the fitted titration curve to the absorption at 470 nm.

~~Using the same spectrophotometric method, K_d for dUMP binding to ThyX from *T. maritima* was previously estimated at 0.03 μM[19] and 0.4 μM[36] determined at room temperature and 60ºC, respectively. In contrast, K_d for dUMP binding to ThyX from *Mtb* obtained in this study at room temperature is 3.8 μM, suggesting that the two proteins may be significantly different and ThyX from *T. maritima* may be a poor model to study the function and ligand interactions of ThyX from *Mtb* and vice versa.~~

The ionization state of the C8-C1 inhibitor

By analogy to 5F-dUMP, we propose that a molecule with an increased acidity compared to dUMP, such as 2-OH NQs, and having the same interactions with ThyX should bind to ThyX more strongly than the natural dUMP substrate. First, we used UV-vis spectroscopy to determine the protonation state of the C8-C1 ligand in solution. In the previous study, we observed that the C8-C1 ligand has a halochromic property as its solution changes the color with the pH change.[5] Figure 2 shows the absorption spectra of the molecule C8-C1 measured at different pH. These optical spectra are in a good agreement with the published spectra experimentally determined for other derivatives of 2-hydroxy NQ.[37] To determine pK_a of C8-C1, the absorption intensity at 470 nm at different pH values was fitted to the Henderson–Hasselbalch equation, as shown in Figure 2. The experimental pK_a of the C8-C1 inhibitor in solution was determined to correspond to 5.5±0.1 units. This value is close to pK_a of 5.75 units reported previously for 2-hydroxy-3-(3-methyl-1-butenyl)-1,4-naphthoquinone in water: ethanol (1:1) solution.[37]

To determine the protonation state of the C8-C1 ligand bound to the active site of the ThyX, we used alchemical free energy simulations ~~(Table 1)~~. The results are given in Table 1. The computed free energy in the protein relative to the solvent is -8.1 (SD 0.2) kcal·mol^{-1} indicating that the protein strongly stabilizes the ionized ligand. This value is very close to the deprotonation free energy computed for dUMP -8.6 kcal·mol^{-1} and reflects the fact that the O2 group of C8-C1, similar to N3 of dUMP, closely interacts with Arg199 in 100 ns Molecular Dynamics (MD) simulations as well as in the crystal structure. The averaged distance between the O2 atom of C8-C1 and the NH1 atom of Arg199 in MD simulations is 2.8 Å, in agreement with the crystal structure (2.9 Å), as shown in Figure 1. The ionic interaction between the 2-O$^-$ group and Arg199 is strengthened by desolvation in the binding pocket. Using Equation 1 and the experimental pK_a value of 5.5 units in solvent, pK_a of the 2-hydroxyl group of C8-C1 inside ThyX is estimated to be ~ -0.5 units. In these calculations, it was assumed that the protein does not change the conformation upon pH change. However, extreme pH variations can induce strong conformational changes including protein unfolding, but such changes are difficult to take into account in simulations and are beyond the goal of the present study.

To rationalize the low pK_a value of C8-C1 in the ThyX complex, we computed the deprotonation free

energy of the 2-OH group with Arg199 deprotonated on NH1. The deprotonation free energy relative to solvent is 1.6 kcal·mol^{-1} (SD 0.7 kcal·mol^{-1}) with Arg199 deprotonated, in contrast to computed -8.1 kcal·mol^{-1} with Arg199 protonated. Overall, the interaction with Arg199 strongly decreases pK_a of the 2-OH group in the ThyX complex. We also computed the deprotonation free energy of Arg199 in the presence and absence of the charged C8-C1 ligand. The computed deprotonation free energy of Arg199 relative to solvent is 5.6±2.5 kcal·mol^{-1}, strongly favoring the protonated form. Thus, Arg199 is always in the cationic form, in agreement with the notion that arginines strongly prefer to be protonated even in the hydrophobic environment.[38] Finally, this deprotonation free energy of Arg199 in the ThyX protein without the C8-C1 ligand is 0.9±1.3 kcal·mol^{-1} indicating that the upshifted pK_a of Arg199 in the ThyX complex can be explained by the strong electrostatic interaction with C8-C1 and without the bound ligand Arg199 has a pK_a value as in the solvent.

Identification of benzoate as a weak inhibitor of ThyX

Based on these insights we propose that a competitive inhibitor to dUMP should be ionized in ThyX similar to dUMP, 5F-dUMP, and C8-C1 to be able to make strong electrostatic interactions with Arg199. Such an inhibitor should also be able to interact with the isoalloxazine group of FAD and fill the hydrophobic cavity next to it. As an example, we propose that a simple molecule, benzoate, in principle, fulfills these requirements. This molecule was first tested in MD simulations showing that benzoate indeed makes stable interactions during the 100 ns MD simulations with Arg199 and stacking interactions with the flavin rings. Deprotonated benzoic acid was manually positioned in place of 5F-dUMP in the model built using the crystal structure (PDB reference code 3GWC) as described in the Methods section. In this orientation, the carboxylic group interacts with the guanidium group of Arg199, as shown in Figure 3, while the benzene group makes stacking interactions with the flavin group of FAD. The root mean square deviation (RMSD) for the unrestrained protein backbone atoms relative to the position in the experimental structure (PDB code 3GWC) was 0.59 Å. The RMS deviation for the benzoate ligand relative to its average position is 0.58 Å in the MD simulations and is comparable to the RMS deviations observed for the 5F-dUMP ligand in simulations with ThyX (RMSD: 0.50 Å), demonstrating the convergence. Overall, the configuration shown in Figure 3 was stable in the 100 ns MD simulations. In particular, the benzene ring made the π–π stacking interaction with the flavin rings. The average distances between the oxygens of the benzoate ligand and the NH nitrogens of Arg199 were 2.6-3.2 Å demonstrating that the strong ionic interactions with Arg199 were maintained during the MD simulations. Overall, the stacking interactions between benzoate and flavin and ionic interactions with Arg199 are similar to the observed interactions for dUMP and C8-C1 in the crystal structures in complex with ThyX. To assess the strength of interactions between benzoate and ThyX, the binding free energy difference between benzoate and C8-C1 was computed using the Linear Interaction Energy (LIE) method. The results of these calculations are given in Table S10. The computed free energy difference between benzoate and C8-C1 binding to ThyX from *Mtb* is 1.9 (SD: 1.2) kcal·mol^{-1} favoring C8-C1 binding.

The binding of benzoate was further confirmed by spectrophotometric titration experiments showing that, similar to other ligands, the absorption of the protein decreases at 450 nm, as shown in Figure 3. The estimated K_d over two independent measurements was 72.7 μM, demonstrating that benzoate is a relatively weak inhibitor of ThyX. Using the previous experimental estimate for C8-C1 binding to ThyX of 4.5 μM, the experimental binding free energy difference between C8-C1 and benzoate to ThyX from *Mtb* is 1.7 kcal·mol^{-1} in good agreement with the computed binding free energy difference of 1.9 kcal·mol^{-1}. This weak inhibitory activity could partly explain the fact that benzoic acid in significant concentrations affects the growth of *Mtb* cells as demonstrated previously.[39] These results encourage benzoate as the candidate scaffold for ThyX inhibitors.

Figure 3. (A) Structure of the complex between benzoate and ThyX observed in MD simulations with indicated important distances averaged over MD simulations. (B) Spectrophotometric titration of benzoate. The structural figure was prepared with the Pymol.[34]

Discussion

Overall, the results of the present study indicate, in agreement with the earlier work, that ThyX stabilizes the ionized uracil of dUMP, while the protonated neutral form is unlikely to bind to ThyX. We propose that the acidity at the N3 atom of dUMP can affect interactions with ThyX, since the ionized form is more readily available for binding. Indeed, experiments and simulations here demonstrate that 5F-dUMP, which has pK_a at the N3 atom of 8 units in solution, interacts stronger with ThyX. The experimental and simulation results obtained in this work also show that the 2-OH-NQ inhibitor mimicking the natural dUMP is deprotonated at O2 in the ThyX complex and has a very similar mode of interaction with Arg199. The C8-C1 pK_a value in solution of 5.5 pH units is lower than the pK_a of N3 of dUMP (9.3 pH units[31]). Thus, in the case of 2-OH naphthoquinones, there is no free energy penalty associated with the deprotonation of the 2-OH group upon binding in contrast to the natural dUMP substrate. In summary, the results obtained in this work show that the pK_a of the natural dUMP substrate and 2-OH-NQs in solution strongly modulates their binding affinity to ThyX. These novel atomistic details explain the selective mechanism of 2-OH-NQs to ThyX and will facilitate the rational design of new antibiotics exploiting the unique reaction mechanism of ThyX enzymes.

Based on these insights we propose that a competitive inhibitor to dUMP should be ionized in ThyX similar to dUMP, 5F-dUMP, and C8-C1 to be able to make strong electrostatic interactions with Arg199. Such an inhibitor should also be able to interact with the isoalloxazine group of FAD. As an example, we propose that a simple molecule, benzoate, in principle, fulfills these requirements. During the long MD simulations benzoate indeed makes stable interactions with Arg199 and stacking interactions with the flavin rings. The binding of benzoate was further confirmed by spectrophotometric titration experiments showing that benzoate binds to ThyX from *Mtb* with K_d of 72.7 μM. This weak inhibitory activity could partly explain the fact that benzoic acid

in significant concentrations affects the growth of *Mtb* cells demonstrated previously.[39] These results encourage benzoate as the scaffold for future ThyX inhibitors. Importantly, using the spectrophotometric method, it was shown that K_d for dUMP binding to ThyX from *Mtb* is at least two orders magnitude higher than K_d reported in the previous study for dUMP binding to ThyX from *T. maritima*.[19] ~~This demonstrates that the two proteins accomplishing the same function may be significantly different, and ThyX from *T. maritima* may not be a suitable model to study the function and ThyX from *Mtb*.~~

Finally, the results of this work may also be pertinent to other flavoenzymes such as D-amino acid oxidase, where similar to ThyX, ionic interactions with arginine and stacking interactions with flavin explain inhibition by small molecules including benzoate that was identified in this work as a weak inhibitor of ThyX.[40] Importantly, the results of this work also correlate with the molecular basis of the antimalarial drug, atovaquone inhibition of the cytochrome bc1 complex, discovered in a very recent study.[41] In particular, atovaquone, a derivative of 2-OH-NQ with a substituent at position 3, is structurally very similar to C8-C1 and inhibits cytochrome bc1 complex via strong ionic interactions with a conserved protonated histidine,[41] suggesting that for the class of molecules based on 2-OH-NQ ionic interactions with protein targets may be common.

METHODS AND MATERIALS

Protein expression and purification

The *Mycobacterium tuberculosis* ThyX enzyme was expressed in *E. coli* BL21(DE3)/pLysS strains containing the recombinant pET24d plasmid carrying the *M. tuberculosis* H37Rv *thyX* gene (Rv2754c) as previously described.[42] Before the purification step, 200 µM of flavin-adenine dinucleotide (FAD) cofactor was added to the supernatant after the lysis step to increase the amount of FAD bound to the *Mtb* ThyX protein. The solubilized protein extract was loaded on a Hi-Trap Talon 5 mL column (GE Healthcare) previously equilibrated with 10-bed volumes of the equilibration buffer containing 30 mM Hepes and 300 mM NaCl at pH 8.0. The column was subsequently washed with 10-bed volumes of the same equilibration buffer, and the His-tagged ThyX protein was eluted with 5-bed volumes elution buffer (30 mM Hepes pH 8.0, 300 mM NaCl, 500 mM imidazole). The fractions containing *Mtb* ThyX enzyme were pooled, buffer-exchanged on Econo-Pac PD-10 columns (Bio-rad) with the equilibration buffer, concentrated to a final concentration of 480 µM, and stored at -20°C for further use. The measured absorbance of FAD bound to *Mtb* ThyX at 450 nm showed a ratio FAD to ThyX of 1 to 3 for the purified *Mtb* ThyX chain.

Spectrophotometric titrations

UV-vis spectra of the inhibitor C8-C1 in solution were obtained using a NanoDrop microvolume spectrophotometer. Measurements were performed in the pH range between 4.2 and 7.2 with steps of 0.6 pH units. Different pH values were obtained by mixing 0.1 M citric acid and 0.2 M disodium hydrogen phosphate solutions according to McIlvaine.[43] The pK_a value for C8-C1 was determined by fitting the intensity of

absorption at 470 nm at different pH values to the Henderson–Hasselbalch equation.

Spectrophotometric binding experiments were performed using a Shimadzu UV-Vis 1700 scanning spectrophotometer at 298 K; 48 µM enzyme in 50 mM HEPES at pH 8 with the NaCl concentration of 30 mM. The FAD:ThyX concentration was 16 µM as calculated using the absorption at 450 nm and the extinction coefficient of flavin. Absorbance spectra were measured with a 2-5 minute delay after each addition. The data were fitted to the tight-binding or Morrison's expression 1:

$$\Delta A = \frac{\Delta\varepsilon_{max}\, l}{2}\left(E_0 + L_0 + K_d - \sqrt{(E_0 + L_0 + K_d)^2 - 4E_0L_0}\right), \quad \text{[Eq. 1]}$$

where $\Delta\varepsilon_{max}$ is the maximal change in extinction coefficient; l is the path length; E_0 and L_0 are the total enzyme and ligand concentration, respectively.[44]

Molecular Dynamics simulations

The crystal structure of thymidylate synthase ThyX in complex with the inhibitor, 2-hydroxy-3-(4-methoxybenzyl)naphthalene-1,4-dione (C8-C1) and a flavin adenine dinucleotide (FAD) cofactor was obtained from the Protein Data Bank (PDB), entry 4FZB.[5] This ThyX protein is from *Paramecium bursaria* Chlorella virus 1 (PBCV-1). Simulations of 5F-dUMP and dUMP in complex with ThyX were started using the PDB structure, entry 3GWC,[32] corresponding to 5F-dUMP in complex with ThyX from *Mtb*. We use residue numbering that corresponds to ThyX from *Mtb*; where needed the corresponding numbers for ThyX from PBCV-1 are also provided. The simulations included protein residues within a 24 Å sphere, centered on one of four FAD cofactors in the crystal structure. Protonation states of histidines were assigned by visual inspection and ideal stereochemistry; protonation states of other residues were assigned using PROPKA.[45-46] Thus, Glu92 was in the neutral form, which is also consistent with the short distance of 2.6 Å between the Oε oxygen of Glu92 and the phosphate oxygen of 5F-dUMP observed in the crystal structure 3GWC. The dUMP or 5F-dUMP ligands were assumed to be deprotonated at N3 in accord with previous NMR measurements,[19] in all calculations unless otherwise stated. Protein atoms between 20 and 24 Å from the sphere's center were harmonically restrained to their experimentally determined positions. The spherical model allowed to focus on the relevant degrees of freedom around the ThyX binding site, while distant groups beyond 24 Å were not included as they were expected not to contribute to interactions with the ligands. To test this conjecture, the contribution of protein residues beyond 24 Å to the binding free energy of C8-C1 was estimated using the Poisson-Boltzmann free energy as described in the Supporting Information. Overall, the contribution of distant protein residues to ligand-binding free energy was found to be very small, less than 0.1 kcal·mol^{-1}. To model C8-C1 in complex with ThyX from *Mtb*, the C8-C1 ligand from the crystal structure from PBCV-1 was retained after superimposing the crystal structures from ThyX and PBCV-1, PDB entries 4FZB and 3GWC, using the protein backbone atoms. The geometry of the ligand was then energetically minimized with the protein and FAD atoms fixed to their experimental positions using the CHARMM software.[47]

In addition to crystal waters, a 75-Å cubic box of water was overlaid, and waters overlapping the protein,

ligands, and crystal water molecules were removed. Periodic boundary conditions were assumed; i.e. the entire 75-Å box was replicated periodically in all directions. All long-range electrostatic interactions were computed efficiently by the particle mesh Ewald method,[48] and the appropriate number of potassium counterions were included to render the system electrically neutral. MD simulations were performed at constant room temperature and pressure, after 200 ps of equilibration. The CHARMM36 force field was used for the protein[49-50] and the TIP3P model for water.[51-53] The 2-OH NQs were modeled using the force field model specifically developed as part of this work. In particular, lawsone, quinone, 3-methyl-2-hydroxy-1,4-naphthoquinone, C8-C1, 3-hydroxy-2-methyl-4H-chromen-4-one were parametrized. Details of the parametrization and force field parameters are given in the Supporting Information. The FAD cofactor was modelled using a recently developed force field model.[54] Calculations were done with the NAMD and CHARMM programs.[47, 55] MD simulations of the protein complexes were continued for 100 nanoseconds.

Protonation Free Energy ~~Perturbation (FEP)~~ calculations

The alchemical free energy ~~perturbation~~ method was used to calculate protonation free energy of dUMP, 2-hydroxy naphthoquinone, and Arg199 in the ThyX complex.[56] The protein system was the same as described above. Solvent simulations included a compound solvated in a cubic box of water so that the minimum distance between the compound atoms and the edge of the system was 12 Å. With this setup, the protein or compounds are well solvated, and thus the contribution of artifacts of the periodic boundary conditions to free energy changes due to perturbed solute charges are expected to be small as it was demonstrated in the previous work.[56] The atomic charges of a specific group of interest were linearly scaled using a coupling parameter λ from the charges of the protonated form to the charges of the deprotonated form. To obtain the free energy of the protonated form relative to the deprotonated form, we performed MD simulations at a series of λ values: 0.0, 0.2, 0.4, 0.6, 0.8, and 1.0, called windows. Free energy derivatives, $\partial G/\partial\lambda = \langle \partial U/\partial\lambda \rangle_\lambda$, were computed numerically and averaged over 100 structures from a window simulation. The corresponding free energy was then obtained by thermodynamic integration (TI). Each window simulation continued for 4 ns. To estimate the numerical error of the simulations, three forward-backward runs were consequently performed. Thus, to obtain a free energy value in solvent or in the protein complex, in total 144 ns of MD free energy simulations were performed with the NAMD program.[55] The corresponding free energy change was computed both in the protein complex and for the model compound alone in solution. The pK_a shift due to the protein environment has the form:

$$\mathrm{p}K_\mathrm{a}^{prot} - \mathrm{p}K_\mathrm{a}^{solv} = (\Delta G^{prot} - \Delta G^{solv})/2.303/RT\ , \quad \text{[Eq. 2]}$$

where ΔG^{prot} and ΔG^{solv} are free energy change in the protein and solvent, respectively; R is the gas constant and T is temperature. Calculations were repeated in vacuum using Langevin dynamics as implemented in NAMD.[55] The free energies in vacuum were then subtracted from the values in solvent and protein to remove artificial contributions arising from the use of the force field model. ~~It should be noted that when the free energy in the protein relative to solvent is considered in Equation 2, the free energy in vacuum cancels out.~~

Binding Free Energy calculations

The alchemical free energy method was used to calculate the binding free energy difference between dUMP and 5F-dUMP. These calculations rely on the thermodynamic cycle as described in the previous works.[57-58] The corresponding work was derived from a thermodynamic integration formula.[58] The electrostatic contribution due to perturbing charges on atoms and the van der Waals (vdW) contribution were computed separately. The vdW contribution was computed using the free energy method implemented in NAMD.[55] The vdW potential was shifted with the coefficient of four to ensure that the potential is finite for small values of the decoupling parameters.[59] The electrostatic contribution to the binding free energies was computed using the same protocol described above for the protonation free energy calculations.

To calculate binding free energy differences between the C8-C1 and benzoate ligands the linear interaction energy approach was used.[60-61] In this method the binding free energy is approximated as the change in the electrostatic and van der Waals interaction energy between the ligand and its environment upon complex formation. The energy contributions to the binding free energy are scaled by weighting factors using the following equation:

$$\Delta G = \alpha\, \Delta E^{Elec} + \beta\, \Delta E^{vdW} + \gamma\,, \quad \text{[Eq. 3]}$$

where $\alpha = 0.5$, $\beta = 0.16$; and γ cancels out when binding free energy difference is computed.[61-62] The electrostatic and vdW interaction energies were averaged over 500 conformations total drawn from MD simulations in the protein complex and in solvent at every 200 ps. The error was estimated as the standard deviation of energies averaged over five consecutive 20-ns simulations obtained from the entire 100-ns MD simulation for each protein complex and ligand in solvent.

Supporting Information

Details of the force field model development for NQs, results of binding free energy calculations with the LIE method, the computed effect of distant protein residues on the ligand binding, and the force field parameters (PDF)

Author Contributions

HM designed research; performed research; analyzed data; and wrote the manuscript. HFB performed research; analyzed data. AA designed research; performed research; analyzed data; and wrote the manuscript

Acknowledgments

This work was supported by grant ANR-18-CE44-0002. This work was performed using HPC resources from GENCI-CINES (Grant 2018-A0040710436). We thank Marten Vos and Ursula Liebl for the helpful discussions.

Competing interests

The authors declare no competing interests.

References

1. Tandon, V. K.; Kumar, S., Recent development on naphthoquinone derivatives and their therapeutic applications as anticancer agents. *Expert Opin. Ther. Pat.* **2013,** *23* (9), 1087-1108.
2. Benites, J.; Valderrama, J. A.; Bettega, K.; Pedrosa, R. C.; Calderon, P. B.; Verrax, J., Biological evaluation of donor-acceptor aminonaphthoquinones as antitumor agents. *Eur. J. Med. Chem.* **2010,** *45* (12), 6052-7.
3. Pereyra, C. E.; Dantas, R. F.; Ferreira, S. B.; Gomes, L. P.; Silva-Jr, F. P., The diverse mechanisms and anticancer potential of naphthoquinones. *Cancer Cell Int.* **2019,** *19*, 207.
4. Skouloubris, S.; Djaout, K.; Lamarre, I.; Lambry, J. C.; Anger, K.; Briffotaux, J.; Liebl, U.; de Reuse, H.; Myllykallio, H., Targeting of Helicobacter pylori thymidylate synthase ThyX by non-mitotoxic hydroxy-naphthoquinones. *Open biology* **2015,** *5* (6), 150015.
5. Basta, T.; Boum, Y.; Briffotaux, J.; Becker, H. F.; Lamarre-Jouenne, I.; Lambry, J. C.; Skouloubris, S.; Liebl, U.; Graille, M.; van Tilbeurgh, H.; Myllykallio, H., Mechanistic and structural basis for inhibition of thymidylate synthase ThyX. *Open biology* **2012,** *2* (10), 120120.
6. Moreira, C. S.; Silva, A. C. J. A.; Novais, J. S.; Sá Figueiredo, A. M.; Ferreira, V. F.; da Rocha, D. R.; Castro, H. C., Searching for a potential antibacterial lead structure against bacterial biofilms among new naphthoquinone compounds. *J. Appl. Microbiol.* **2017,** *122* (3), 651-662.
7. Mahapatra, A.; Mativandlela, S. P. N.; Binneman, B.; Fourie, P. B.; Hamilton, C. J.; Meyer, J. J. M.; van der Kooy, F.; Houghton, P.; Lall, N., Activity of 7-methyljuglone derivatives against Mycobacterium tuberculosis and as subversive substrates for mycothiol disulfide reductase. *Biorg. Med. Chem.* **2007,** *15* (24), 7638-7646.
8. Futuro, D. O.; Ferreira, P. G.; Nicoletti, C. D.; Borba-Santos, L. P.; Silva, F. C. D.; Rozental, S.; Ferreira, V. F., The Antifungal Activity of Naphthoquinones: An Integrative Review. *An. Acad. Bras. Cienc.* **2018,** *90* (1 Suppl 2), 1187-1214.
9. Polonik, S. G.; Tolkach, A. M.; Stekhova, S. I.; Shentsova, E. B.; Uvarova, N. I., Synthesis of acetylated glycosides of hydroxyjuglones and study of their antifungal activity. *Pharm. Chem. J.* **1992,** *26* (6), 500-502.
10. Staniforth, V.; Wang, S. Y.; Shyur, L. F.; Yang, N. S., Shikonins, phytocompounds from Lithospermum erythrorhizon, inhibit the transcriptional activation of human tumor necrosis factor alpha promoter in vivo. *J. Biol. Chem.* **2004,** *279* (7), 5877-85.
11. Faria, R. X.; Oliveira, F. H.; Salles, J. P.; Oliveira, A. S.; von Ranke, N. L.; Bello, M. L.; Rodrigues, C. R.; Castro, H. C.; Louvis, A. R.; Martins, D. L.; Ferreira, V. F., 1,4-Naphthoquinones potently inhibiting P2X7 receptor activity. *Eur. J. Med. Chem.* **2018,** *143*, 1361-1372.
12. Aminin, D.; Polonik, S., 1,4-Naphthoquinones: Some Biological Properties and Application. *Chem. Pharm. Bull. (Tokyo)* **2020,** *68* (1), 46-57.
13. Myllykallio, H.; Sournia, P.; Heliou, A.; Liebl, U., Unique Features and Anti-microbial Targeting of Folate- and Flavin-Dependent Methyltransferases Required for Accurate Maintenance of Genetic Information. *Frontiers in microbiology* **2018,** *9*, 918.
14. Myllykallio, H.; Lipowski, G.; Leduc, D.; Filee, J.; Forterre, P.; Liebl, U., An alternative flavin-dependent mechanism for thymidylate synthesis. *Science* **2002,** *297* (5578), 105-7.
15. Kuhn, P.; Lesley, S. A.; Mathews, II; Canaves, J. M.; Brinen, L. S.; Dai, X.; Deacon, A. M.; Elsliger, M. A.; Eshaghi, S.; Floyd, R.; Godzik, A.; Grittini, C.; Grzechnik, S. K.; Guda, C.; Hodgson, K. O.; Jaroszewski, L.; Karlak, C.; Klock, H. E.; Koesema, E.; Kovarik, J. M.; Kreusch, A. T.; McMullan, D.; McPhillips, T. M.; Miller, M. A.; Miller, M.; Morse, A.; Moy, K.; Ouyang, J.; Robb, A.; Rodrigues, K.; Selby, T. L.; Spraggon, G.; Stevens, R. C.; Taylor, S. S.; van den Bedem, H.; Velasquez, J.; Vincent, J.; Wang, X.; West, B.; Wolf, G.; Wooley, J.; Wilson, I. A., Crystal structure of thy1, a thymidylate synthase complementing protein from Thermotoga maritima at 2.25 A resolution. *Proteins* **2002,** *49* (1), 142-5.
16. Sampathkumar, P.; Turley, S.; Ulmer, J. E.; Rhie, H. G.; Sibley, C. H.; Hol, W. G., Structure of the Mycobacterium tuberculosis flavin dependent thymidylate synthase (MtbThyX) at 2.0A resolution. *J. Mol. Biol.* **2005,** *352* (5), 1091-104.
17. Sampathkumar, P.; Turley, S.; Sibley, C. H.; Hol, W. G., NADP+ expels both the co-factor and a substrate analog from the Mycobacterium tuberculosis ThyX active site: opportunities for anti-bacterial drug design. *J. Mol. Biol.* **2006,** *360* (1), 1-6.
18. Mishanina, T. V.; Yu, L.; Karunaratne, K.; Mondal, D.; Corcoran, J. M.; Choi, M. A.; Kohen, A., An unprecedented mechanism of nucleotide methylation in organisms containing thyX. *Science* **2016,** *351* (6272), 507-510.
19. Stull, F. W.; Bernard, S. M.; Sapra, A.; Smith, J. L.; Zuiderweg, E. R. P.; Palfey, B. A., Deprotonations in the Reaction of Flavin-Dependent Thymidylate Synthase. *Biochemistry* **2016,** 55 (23), 3261-3269.
20. Kogler, M.; Vanderhoydonck, B.; De Jonghe, S.; Rozenski, J.; Van Belle, K.; Herman, J.; Louat, T.; Parchina, A.; Sibley, C.; Lescrinier, E.; Herdewijn, P., Synthesis and evaluation of 5-substituted 2'-deoxyuridine monophosphate analogues as inhibitors of flavin-dependent thymidylate synthase in Mycobacterium tuberculosis. *J. Med. Chem.* **2011,** *54* (13), 4847-62.
21. Kogler, M.; Busson, R.; De Jonghe, S.; Rozenski, J.; Van Belle, K.; Louat, T.; Munier-Lehmann, H.; Herdewijn, P., Synthesis and evaluation of 6-aza-2'-deoxyuridine monophosphate analogs as inhibitors of thymidylate synthases, and as substrates or inhibitors of thymidine monophosphate kinase in Mycobacterium tuberculosis. *Chem. Biodivers.* **2012,** *9* (3), 536-56.
22. Abu El Asrar, R.; Margamuljana, L.; Klaassen, H.; Nijs, M.; Marchand, A.; Chaltin, P.; Myllykallio, H.; Becker, H. F.; De

Jonghe, S.; Herdewijn, P.; Lescrinier, E., Discovery of a new Mycobacterium tuberculosis thymidylate synthase X inhibitor with a unique inhibition profile. *Biochem. Pharmacol.* **2017,** *135*, 69-78.
23. Fivian-Hughes, A. S.; Houghton, J.; Davis, E. O., Mycobacterium tuberculosis thymidylate synthase gene thyX is essential and potentially bifunctional, while thyA deletion confers resistance to p-aminosalicylic acid. *Microbiology* **2012,** *158* (Pt 2), 308-18.
24. Esra Onen, F.; Boum, Y.; Jacquement, C.; Spanedda, M. V.; Jaber, N.; Scherman, D.; Myllykallio, H.; Herscovici, J., Design, synthesis and evaluation of potent thymidylate synthase X inhibitors. *Bioorg. Med. Chem. Lett.* **2008,** *18* (12), 3628-31.
25. Singh, V.; Brecik, M.; Mukherjee, R.; Evans, J. C.; Svetlikova, Z.; Blasko, J.; Surade, S.; Blackburn, J.; Warner, D. F.; Mikusova, K.; Mizrahi, V., The complex mechanism of antimycobacterial action of 5-fluorouracil. *Chem. Biol.* **2015,** *22* (1), 63-75.
26. Parchina, A.; Froeyen, M.; Margamuljana, L.; Rozenski, J.; De Jonghe, S.; Briers, Y.; Lavigne, R.; Herdewijn, P.; Lescrinier, E., Discovery of an acyclic nucleoside phosphonate that inhibits Mycobacterium tuberculosis ThyX based on the binding mode of a 5-alkynyl substrate analogue. *ChemMedChem* **2013,** *8* (8), 1373-83.
27. McGuigan, C.; Derudas, M.; Gonczy, B.; Hinsinger, K.; Kandil, S.; Pertusati, F.; Serpi, M.; Snoeck, R.; Andrei, G.; Balzarini, J.; McHugh, T. D.; Maitra, A.; Akorli, E.; Evangelopoulos, D.; Bhakta, S., ProTides of N-(3-(5-(2′-deoxyuridine))prop-2-ynyl)octanamide as potential anti-tubercular and anti-viral agents. *Bioorg. Med. Chem.* **2014,** *22* (9), 2816-24.
28. Luciani, R.; Saxena, P.; Surade, S.; Santucci, M.; Venturelli, A.; Borsari, C.; Marverti, G.; Ponterini, G.; Ferrari, S.; Blundell, T. L.; Costi, M. P., Virtual Screening and X-ray Crystallography Identify Non-Substrate Analog Inhibitors of Flavin-Dependent Thymidylate Synthase. *J. Med. Chem.* **2016,** *59* (19), 9269-9275.
29. Djaout, K.; Singh, V.; Boum, Y.; Katawera, V.; Becker, H. F.; Bush, N. G.; Hearnshaw, S. J.; Pritchard, J. E.; Bourbon, P.; Madrid, P. B.; Maxwell, A.; Mizrahi, V.; Myllykallio, H.; Ekins, S., Predictive modeling targets thymidylate synthase ThyX in Mycobacterium tuberculosis. *Sci. Rep.* **2016,** *6*.
30. Mathews, II; Deacon, A. M.; Canaves, J. M.; McMullan, D.; Lesley, S. A.; Agarwalla, S.; Kuhn, P., Functional analysis of substrate and cofactor complex structures of a thymidylate synthase-complementing protein. *Structure* **2003,** *11* (6), 677-90.
31. Aylward, N. N., Thermodynamic constants of the ionisation of the acid imino-group of uridine 5′-monophosphate and poly-uridylic acid. *Journal of the Chemical Society B: Physical Organic* **1967,** (0), 401-403.
32. Baugh, L.; Phan, I.; Begley, D. W.; Clifton, M. C.; Armour, B.; Dranow, D. M.; Taylor, B. M.; Muruthi, M. M.; Abendroth, J.; Fairman, J. W.; Fox, D., 3rd; Dieterich, S. H.; Staker, B. L.; Gardberg, A. S.; Choi, R.; Hewitt, S. N.; Napuli, A. J.; Myers, J.; Barrett, L. K.; Zhang, Y.; Ferrell, M.; Mundt, E.; Thompkins, K.; Tran, N.; Lyons-Abbott, S.; Abramov, A.; Sekar, A.; Serbzhinskiy, D.; Lorimer, D.; Buchko, G. W.; Stacy, R.; Stewart, L. J.; Edwards, T. E.; Van Voorhis, W. C.; Myler, P. J., Increasing the structural coverage of tuberculosis drug targets. *Tuberculosis (Edinburgh, Scotland)* **2015,** *95* (2), 142-8.
33. Wood, E. J., Data for biochemical research (third edition) by R M C Dawson, D C Elliott, W H Elliott and K M Jones, pp 580. Oxford Science Publications, OUP, Oxford, 1986. £35/$59. ISBN 0-19-855358-7. *Biochemical Education* **1987,** *15* (2), 97-97.
34. *The PyMOL Molecular Graphics System*, Version 1.8; Schrödinger, LLC.
35. *MarvinSketch*, Version 19.13; ChemAxon.
36. Laptenok, S. P.; Bouzhir-Sima, L.; Lambry, J. C.; Myllykallio, H.; Liebl, U.; Vos, M. H., Ultrafast real-time visualization of active site flexibility of flavoenzyme thymidylate synthase ThyX. *Proc. Natl. Acad. Sci. U.S.A.* **2013,** *110* (22), 8924-9.
37. Ossowski, T.; Goulart, M. O. F.; Abreu, F. C. d.; Sant Ana, A. E. G.; Miranda, P. R. B.; Costa, C. d. O.; Liwo, A.; Falkowski, P.; Zarzeczanska, D., Determination of the pKa values of some biologically active and inactive hydroxyquinones. *J. Braz. Chem. Soc.* **2008,** *19*, 175-183.
38. Fitch, C. A.; Platzer, G.; Okon, M.; Garcia-Moreno, B. E.; McIntosh, L. P., Arginine: Its pKa value revisited. *Protein Sci.* **2015,** *24* (5), 752-61.
39. Wade, M. M.; Zhang, Y., Effects of weak acids, UV and proton motive force inhibitors on pyrazinamide activity against Mycobacterium tuberculosis in vitro. *J. Antimicrob. Chemother.* **2006,** *58* (5), 936-41.
40. Hopkins, S. C.; Heffernan, M. L.; Saraswat, L. D.; Bowen, C. A.; Melnick, L.; Hardy, L. W.; Orsini, M. A.; Allen, M. S.; Koch, P.; Spear, K. L.; Foglesong, R. J.; Soukri, M.; Chytil, M.; Fang, Q. K.; Jones, S. W.; Varney, M. A.; Panatier, A.; Oliet, S. H.; Pollegioni, L.; Piubelli, L.; Molla, G.; Nardini, M.; Large, T. H., Structural, kinetic, and pharmacodynamic mechanisms of D-amino acid oxidase inhibition by small molecules. *J. Med. Chem.* **2013,** *56* (9), 3710-24.
41. Birth, D.; Kao, W.-C.; Hunte, C., Structural analysis of atovaquone-inhibited cytochrome bc1 complex reveals the molecular basis of antimalarial drug action. *Nat. Commun.* **2014,** *5* (1), 4029.
42. Ulmer, J. E.; Boum, Y.; Thouvenel, C. D.; Myllykallio, H.; Sibley, C. H., Functional analysis of the Mycobacterium tuberculosis FAD-dependent thymidylate synthase, ThyX, reveals new amino acid residues contributing to an extended ThyX motif. *J. Bacteriol.* **2008,** *190* (6), 2056-64.
43. McIlvaine, T. C., A BUFFER SOLUTION FOR COLORIMETRIC COMPARISON. *J. Biol. Chem.* **1921,** *49* (1), 183-186.
44. Morrison, J. F., Kinetics of the reversible inhibition of enzyme-catalysed reactions by tight-binding inhibitors. *Biochim. Biophys. Acta* **1969,** *185* (2), 269-86.
45. Olsson, M. H.; Sondergaard, C. R.; Rostkowski, M.; Jensen, J. H., PROPKA3: Consistent Treatment of Internal and Surface Residues in Empirical pKa Predictions. *J. Chem. Theory Comput.* **2011,** *7* (2), 525-37.
46. Dolinsky, T. J.; Nielsen, J. E.; McCammon, J. A.; Baker, N. A., PDB2PQR: an automated pipeline for the setup of Poisson-Boltzmann electrostatics calculations. *Nucleic Acids Res.* **2004,** *32* (Web Server issue), W665-7.
47. Brooks, B. R.; Brooks, C. L.; Mackerell, A. D.; Nilsson, L.; Petrella, R. J.; Roux, B.; Won, Y.; Archontis, G.; Bartels, C.; Boresch, S.; Caflisch, A.; Caves, L.; Cui, Q.; Dinner, A. R.; Feig, M.; Fischer, S.; Gao, J.; Hodoscek, M.; Im, W.; Kuczera, K.;

Lazaridis, T.; Ma, J.; Ovchinnikov, V.; Paci, E.; Pastor, R. W.; Post, C. B.; Pu, J. Z.; Schaefer, M.; Tidor, B.; Venable, R. M.; Woodcock, H. L.; Wu, X.; Yang, W.; York, D. M.; Karplus, M., CHARMM: the biomolecular simulation program. *J. Comp. Chem.* **2009,** *30* (10), 1545-614.
48. Darden, T., Treatment of Long-Range Forces and Potential. In *Computational Biochemistry & Biophysics*, Becker, O. M.; MacKerell, A. D., Jr; Roux, B.; Watanabe, M., Eds. Marcel Dekker, NY.: 2001.
49. Best, R. B.; Zhu, X.; Shim, J.; Lopes, P. E. M.; Mittal, J.; Feig, M.; MacKerell, A. D., Optimization of the Additive CHARMM All-Atom Protein Force Field Targeting Improved Sampling of the Backbone ϕ, ψ and Side-Chain χ1 and χ2 Dihedral Angles. *J. Chem. Theory Comput.* **2012,** *8* (9), 3257-73.
50. Huang, J.; MacKerell, A. D., Jr., CHARMM36 all-atom additive protein force field: validation based on comparison to NMR data. *J. Comput. Chem.* **2013,** *34* (25), 2135-45.
51. Jorgensen, W.; Chandrasekar, J.; Madura, J.; Impey, R.; Klein, M., Comparison of simple potential functions for simulating liquid water. *J. Chem. Phys.* **1983,** *79*, 926-35.
52. Mackerell, A. D.; Bashford, D.; Bellott, M.; Dunbrack, R. L.; Evanseck, J.; Field, M. J.; Fischer, S.; Gao, J.; Guo, H.; Ha, S.; Joseph, D.; Kuchnir, L.; Kuczera, K.; Lau, F. T. K.; Mattos, C.; Michnick, S.; Ngo, T.; Nguyen, D. T.; Prodhom, B.; Reiher, W. E.; Roux, B.; Smith, J.; Stote, R.; Straub, J.; Watanabe, M.; Wiorkiewicz-Kuczera, J.; Yin, D.; Karplus, M., An all-atom empirical potential for molecular modelling and dynamics study of proteins. *J. Phys. Chem. B* **1998,** *102* (18), 3586-616.
53. Neria, E.; Fischer, S.; Karplus, M., Simulation of activation free energies in molecular systems. *J1 Chem1 Phys.* **1996,** *105*, 1902-1921.
54. Aleksandrov, A., A Molecular Mechanics Model for Flavins. *J. Comput. Chem.* **2019,** *40* (32), 2834-2842.
55. Phillips, J. C.; Braun, R.; Wang, W.; Gumbart, J.; Tajkhorshid, E.; Villa, E.; Chipot, C.; Skeel, R. D.; Kale, L.; Schulten, K., Scalable molecular dynamics with NAMD. *J. Comput. Chem.* **2005,** *26* (16), 1781-802.
56. Lin, Y. L.; Aleksandrov, A.; Simonson, T.; Roux, B., An Overview of Electrostatic Free Energy Computations for Solutions and Proteins. *J. Chem. Theory Comput.* **2014,** *10* (7), 2690-709.
57. Aleksandrov, A.; Simonson, T., Binding of Tetracyclines to Elongation Factor Tu, the Tet Repressor, and the Ribosome: A Molecular Dynamics Simulation Study. *Biochemistry* **2008,** *47* (51), 13594-603.
58. Aleksandrov, A.; Thompson, D.; Simonson, T., Alchemical free energy simulations for biological complexes: powerful but temperamental. *J. Mol. Recognit.* **2010,** *23* (2), 117-27.
59. Beutler, T.; Mark, A.; Schaik, R. v.; Gerber, P.; Gunsteren, W. F. v., Avoiding singularities and numerical instabilities in free energy calculations based on molecular simulations *Chem. Phys. Lett.* **1994,** *222* (6), 529-39.
60. Gutierrez-de-Teran, H.; Aqvist, J., Linear interaction energy: method and applications in drug design. *Methods Mol. Biol.* **2012,** *819*, 305-23.
61. Åqvist, J.; Luzhkov, V. B.; Brandsdal, B. O., Ligand Binding Affinities from MD Simulations. *Acc. Chem. Res.* **2002,** *35* (6), 358-365.
62. Aqvist, J.; Medina, C.; Samuelsson, J. E., A new method for predicting binding affinity in computer-aided drug design. *Protein Eng.* **1994,** *7* (3), 385-91.